Three-dimensional seismic active earth pressure coefficients using upper bound numerical limit analysis: a few preliminary results

Coefficients de poussée tridimensionels séismiques déterminés avec une application numérique du theorème cinématique de l'analyse limite: quelques résultats préliminaires

Santana T., Guerra N.M.C., Antão A.N., Vicente da Silva M.
UNIC, Faculdade de Ciências e Tecnologia, Universidade Nova de Lisboa

ABSTRACT: The finite element program Sublim3D, which is a three-dimensional numerical implementation of the limit analysis upper bound theorem, is applied to determine seismic active horizontal earth pressure coefficients, using the equivalent static forces approach to simulate the seismic effect. The calculations are performed for different width/height ratios of the wall, different seismic horizontal coefficients, two representative values of the friction angle and two values of the soil-to-wall friction ratio. The three-dimensional influence on the seismic active earth pressures is emphasized. The mechanisms involved in the mobilization of the active earth pressures are inferred from the plastic deformation zones determined by the calculations. The ratios between the three-dimensional and two-dimensional seismic horizontal earth pressure coefficients are obtained and found to be, in practical terms, independent on the soil-to-wall friction ratio.

RÉSUMÉ : Le programme aux éléments finis Sublim3D, une implémentation numérique tridimensionnelle du théorème cinématique de l'analyse limite, est appliqué à la détermination des coefficients de poussée horizontal séismiques tridimensionnels, utilisant des forces statiques équivalentes pour simuler l'effet séismique. Les calculs sont réalisés pour différents rapports largeur/hauteur du mûr, différents coefficients séismiques horizontaux, deux valeurs représentatifs de l'angle de frottement du sol et deux valeurs du rapport entre l'angle de frottement sol-structure et l'angle de frottement du sol. L'influence tridimensionnelle dans les coefficients de poussée séismiques est démontrée. Les mécanismes associés à la mobilisation de la poussée des terres sont inférés à partir des zones de déformation plastique déterminés par les calculs. Les rapports entre les coefficients de poussée tridimensionnels et les coefficients bidimensionnels sont déterminés. Leur indépendance de l'angle de frottement entre le sol et le mûr est constatée.

KEYWORDS: three-dimensional seismic active earth pressure coefficients; upper bound limit analysis; finite elements

1 INTRODUCTION.

Static and seismic earth pressures are often determined using plain strain conditions. These conditions are not always adequate, particularly when the width to height ratio of the wall is not very large.

In this paper the finite element program Sublim3D (Vicente da Silva et al. 2012) is used to determine seismic earth pressure coefficients for different width to height ratios.

Sublim3D is a finite element limit analysis program which uses a mixed finite-element formulation that implements the upper-bound theorem. It scales the mechanisms by setting the work rate of the external forces affected by a load parameter equal to one and performs the minimization of the difference between the plastically dissipated work rate and the work rate of the fixed external forces. The code resorts to parallel computing techniques (Vicente da Silva and Antão 2008), thus allowing very large problems to be solved. The program determines strict upper bound approximations of limit loads of geotechnical problems and automatically obtains the mechanisms involved in such loads. An associative flow rule and perfectly plastic behaviour are assumed.

2 DEFINITION OF THE PROBLEM

The geometry of the analyzed problem is represented schematically in Figure 1. The wall is vertical, with width b and height h and assumed as rigid. The free surface of the supported soil is considered horizontal. The soil yield criterion is Mohr-Coulomb, with null cohesion.

For the situation described, a seismic coefficient of active earth pressure, $K_{as\gamma}$, is determined, representing the influence of soil weight; the seismic coefficient of active earth pressures, K_{asq}, representing the influence of constant surcharge loading, is not determined. The active seismic force per unit width $I_{as\gamma}/b$ can be determined through:

$$\frac{I_{as\gamma}}{b} = \frac{1}{2} K_{as\gamma} \gamma h^2 \qquad (1)$$

where γ is the soil unit weight and the other symbols have the meaning previously described.

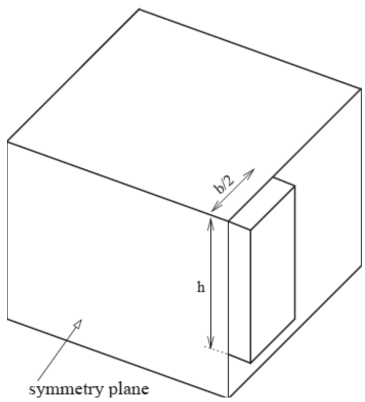

Figure 1. Schematic representation of the geometry of the problem.

The determination of the seismic active earth pressure coefficient was performed for different b/h ratios – 0.25, 0.5, 1, 2, 5 and infinity (two-dimensional), for two values of the soil friction angle, ϕ' – 30 and 40º, and for two values of the soil-to-wall interface friction ratio, δ/ϕ' – 0 and 2/3. The two-dimensional calculations were also performed using the same principles, but considered the more traditional application of the soil pressures directly to the soil, assuming therefore flexible wall.

The loads applied to the soil are: (i) its weight; (ii) a seismic action represented by an equivalent static horizontal unit force, directed towards the wall, equal to $\alpha\gamma$, where α is the seismic horizontal coefficient. No vertical seismic coefficient was considered. The values of α considered in the calculations were: 0, 0.1, 0.2, 0.3, 0.4 and 0.5.

A horizontal force was applied to the wall, centered in width b and at 2h/3 below the soil free surface. The wall can not suffer vertical displacements or slide in the direction of b; it is free to move otherwise. The collapse load determined is $I_{as\gamma h}$, the seismic horizontal active force.

The horizontal component of the seismic active earth pressure coefficient, $K_{as\gamma h}$ can be determined using:

$$K_{as\gamma h} = \frac{I_{as\gamma h}}{\frac{1}{2} b \gamma h^2} \quad (2)$$

The seismic active earth pressure coefficient can be approximately determined using:

$$K_{as\gamma} = \frac{K_{as\gamma h}}{\cos\delta} \quad (3)$$

This equation assumes that friction on the soil-to-wall interface takes place entirely on the vertical direction. In the three-dimensional calculations there is, however, no imposed direction for the mobilization of the soil-to-wall friction and the three-dimensional effect will lead to friction mobilization in the horizontal direction, particularly for lower b/h ratios. For the two dimensional calculations, equation (3) is exact.

All calculations were performed on an eight node cluster of quad-core processor computers, using almost all the available memory. An example of a three dimensional finite element mesh used is presented in Figure 2; in fact, each hexahedron represented in the figure is subdivided into 24 tetrahedral elements. Additionally, interface elements following Krabbenhoft et al. (2005) have been introduced between the rigid wall and the soil, in order to allow considering a friction angle of δ between the two materials. For the case of $\delta/\phi'=0$, a very small value of δ (0.01º) was adopted.

In the two-dimensional calculations the soil was modeled with 3-node triangular finite elements allowing a linear approximation for the velocity fields. As previously mentioned, the wall was not explicitly modeled (it was assumed flexible) and the friction between soil and wall was defined through the inclination of the stresses applied to the soil.

3 PRESENTATION AND ANALYSIS OF RESULTS

Results of the horizontal seismic active earth pressure coefficients are presented in Table 1 and are part of the calculations being performed for a larger range of soil friction angles and soil-to-wall friction ratios. Some of these results are also presented in Figure 3, for the friction angles of 30 and 40º, respectively, and for the two soil-to-wall friction ratios and three horizontal seismic coefficients.

These results show a significant three-dimensional effect of the b/h ratio: for small values of this ratio, there is a significant decrease in the soil seismic horizontal active earth pressure coefficients, with the greater b/h ratios leading to coefficients quite close to the two-dimensional case; in fact for b/h>2 there is small variation in the earth-pressure coefficients, specially for the lower value of the friction angle.

Table 1. Values of the seismic horizontal active earth pressure coefficient, $K_{as\gamma h}$, for different b/h and α, for the two values of the soil friction angle and the two values of the soil-to-wall friction ratio.

ϕ'=30º; δ/ϕ'=0						
b/h	α=0	α=0.1	α=0.2	α=0.3	α=0.4	α=0.5
1/4	0.1454	0.1621	0.1778	0.1975	0.2191	0.2419
1/2	0.2179	0.2481	0.2826	0.3157	0.3591	0.4005
1	0.2715	0.3086	0.3637	0.4308	0.5121	0.5922
2	0.3005	0.3478	0.4190	0.5115	0.6325	0.7734
5	0.3195	0.3789	0.4601	0.5687	0.7138	0.9184
∞ (2D)	0.3314.	0.3997	0.4897	0.6154	0.7970	1.0860

ϕ'=30º; δ/ϕ'=2/3						
b/h	α=0	α=0.1	α=0.2	α=0.3	α=0.4	α=0.5
1/4	0.1178	0.1333	0.1486	0.1677	0.1891	0.2129
1/2	0.1798	0.2070	0.2393	0.2743	0.3176	0.3642
1	0.2267	0.2652	0.3169	0.3808	0.4608	0.5558
2	0.2534	0.3003	0.3671	0.4553	0.5726	0.7295
5	0.2705	0.3256	0.4005	0.5033	0.6525	0.8743
∞ (2D)	0.2820	0.3405	0.4276	0.5459	0.7212	1.0077

ϕ'=40º; δ/ϕ'=0						
b/h	α=0	α=0.1	α=0.2	α=0.3	α=0.4	α=0.5
1/4	0.0730	0.0836	0.0993	0.1020	0.1271	0.1268
1/2	0.1162	0.1438	0.1684	0.1953	0.2244	0.2557
1	0.1643	0.1927	0.2344	0.2834	0.3291	0.3907
2	0.1881	0.2170	0.2781	0.3335	0.4306	0.4964
5	0.2047	0.2511	0.3131	0.3877	0.4965	0.6241
∞ (2D)	0.2170	0.2706	0.3414	0.4364	0.5633	0.7319

ϕ'=40º; δ/ϕ'=2/3						
b/h	α=0	α=0.1	α=0.2	α=0.3	α=0.4	α=0.5
1/4	0.0646	0.0752	0.0860	0.0987	0.1124	0.1272
1/2	0.1035	0.1230	0.1451	0.1707	0.1983	0.2265
1	0.1383	0.1670	0.2046	0.2496	0.2969	0.3572
2	0.1585	0.1941	0.2440	0.3080	0.3882	0.4852
5	0.1710	0.2134	0.2694	0.3473	0.4482	0.5747
∞ (2D)	0.1804	0.2283	0.2924	0.3797	0.5110	0.6613

Figure 4 shows the same results emphasizing the influence of the seismic horizontal coefficient, α. It can be observed from these two charts that $K_{as\gamma h}$ increases with α and that this increase is less important for lower b/h ratios.

In this figure, results from the two-dimensional calculations were also included, as well as the results obtained from Mononobe-Okabe (M-O) method. Both methods give very similar results of $K_{as\gamma h}$ when $\alpha\leq0.2$; for $\alpha>0.2$ the differences between the two methods increase.

As the active coefficient is being determined and the active force is the minimum required to ensure stability, the M-O approximation (also an upper bound solution) is less safe than the numerical results, because they are smaller.

Examples of the mechanisms obtained automatically from the program Sublim3D can be inferred from Figure 5, where the plastic deformation zones in the plan view and in the symmetry plane are shown for the case b/h=1 and $\phi'=30º$, for three values of α – 0, 0.2 and 0.4 and for the two values of the friction ratio of 0 and 2/3.

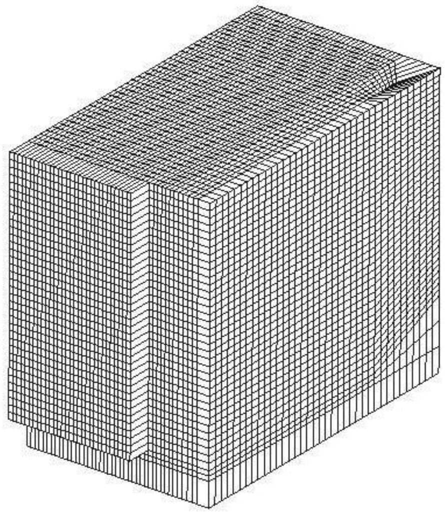

Figure 2. Example of the finite element mesh used in the calculations for b/h=1 (each hexahedron represented in the figure is subdivided into 24 tetrahedral elements).

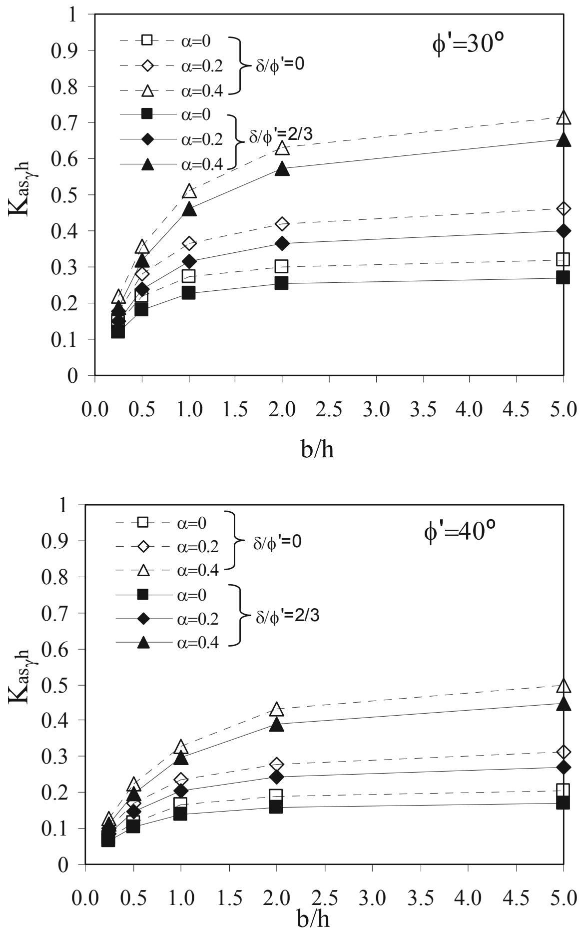

Figure 3. Values of the seismic horizontal active earth pressure coefficient, $K_{as\gamma h}$, as a function of b/h.

It can be observed that the volume of soil involved in the mechanisms is greater for the greater value of α and that it is slightly greater for the greater friction ratio. It can also be seen that for δ/ϕ'=0 and α=0 the mechanism (in the plane of symmetry) is almost planar, whereas the mechanism for δ/ϕ'=2/3 is curved and more complex, although not too far from planar.

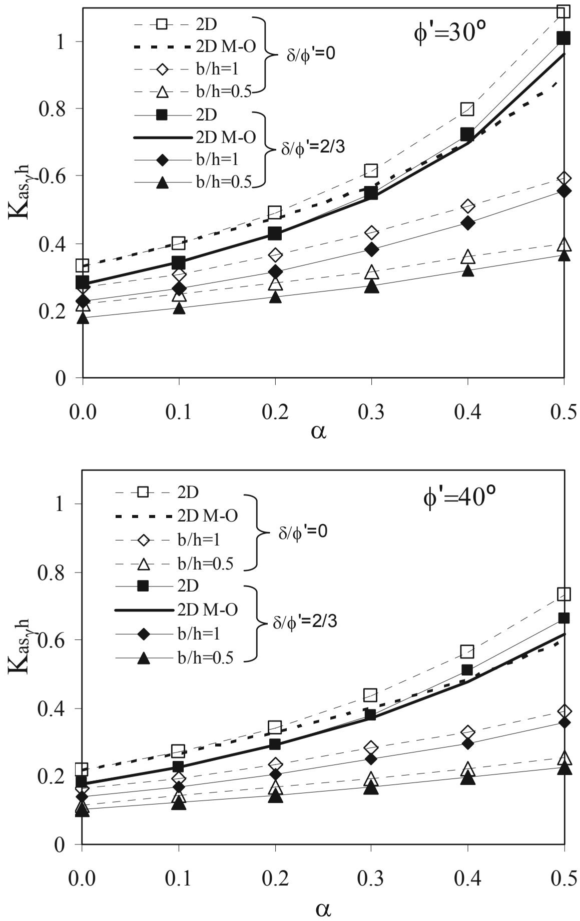

Figure 4. Values of the seismic horizontal active earth pressure coefficient, $K_{as\gamma h}$, as a function of α.

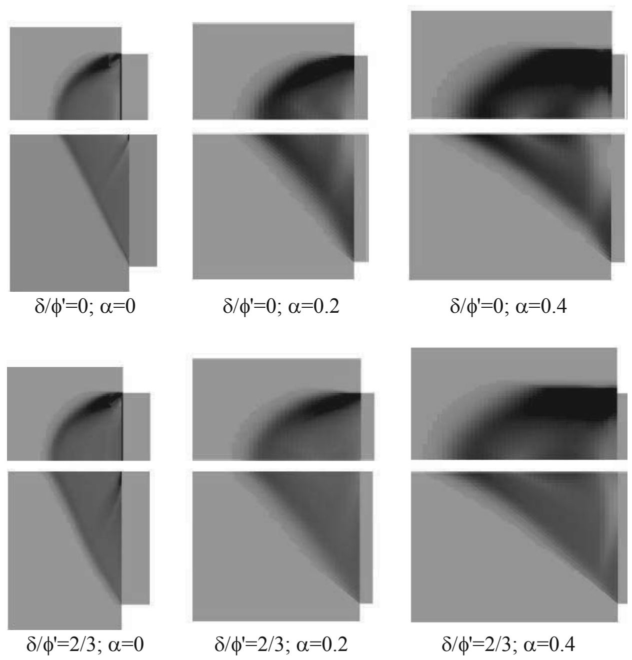

Figure 5. Plastic deformation zones for ϕ'=30º, δ/ϕ'=0 and 2/3, and three values of α – 0, 0.2 and 0.4.

Figure 6 presents the plan views of the plastic deformation zones for ϕ'=30º, δ/ϕ'=2/3 and different b/h ratios and α (for graphical reasons, the case α=0 and b/h=5 is not shown). This figure allows understanding the three-dimensional effect of the b/h ratio on the mechanism involved in the active condition of the soil behind the wall. It can be seen that there is a very clear influence of that ratio on the size of the mechanism and, particularly, on the extension of soil involved in the mechanism, behind the wall, for b/h<2. It can also be seen that the mechanisms show a greater three-dimensional effect for the greater values of α.

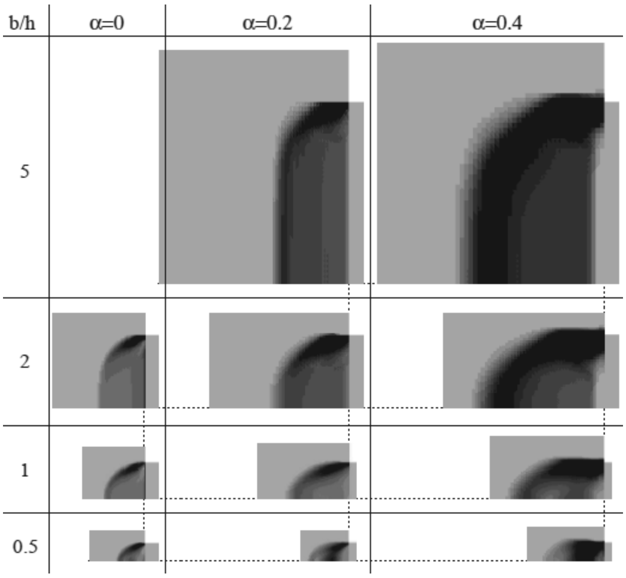

Figure 6. Plan view of the plastic deformation zones for ϕ'=30º, δ/ϕ'=2/3, several b/h ratios – 0.5, 1, 2 and 5 -.and three values of α – 0, 0.2 and 0.4.

Figure 7 represents the values of the ratio $K_{as\gamma h}/K_{as\gamma h2D}$ as a function of b/h, for all cases analyzed. It can be observed, as expected, that this ratio increases with b/h. It can also be observed that the ratios are greater for ϕ'=30º than for ϕ'=40º and greater for the smaller values of α . But, particularly, it can be seen that the ratios of the active earth pressure coefficients are practically independent on the soil-to-wall friction ratio. In fact, the results for δ/ϕ'=0 are superposed with the ones for δ/ϕ'=2/3. This independence on the soil-to-wall friction ratio was also detected in the determination of static passive earth pressure coefficients (Antão et al. 2011).

CONCLUSIONS

A three-dimensional numerical implementation of the limit analysis upper bound theorem, the finite element program Sublim3D, was used to determine seismic active horizontal earth pressure coefficients. The equivalent static forces approach was used to simulate the seismic effect, through a seismic horizontal coefficient The calculations were performed for several width/height ratios of the wall, several seismic horizontal coefficients, two representative values of the friction angle (30 and 40º) and two values of the soil-to-wall friction ratio, δ/ϕ' (0 and 2/3).

The results showed significant three-dimensional effect of the width to height ratio of the wall; in fact, for small values of this ratio, the soil seismic horizontal active earth pressure coefficients are small and for the greater width to height ratios the active earth pressure coefficients are close to the two-dimensional case. It could also be observed that the active earth pressure coefficients increase with the seismic horizontal coefficient and that this increase is less important for lower width to height ratios.

The ratios between the three-dimensional and two-dimensional seismic horizontal earth pressure coefficients were determined and found to be, in practical terms, independent on the soil-to-wall friction ratio.

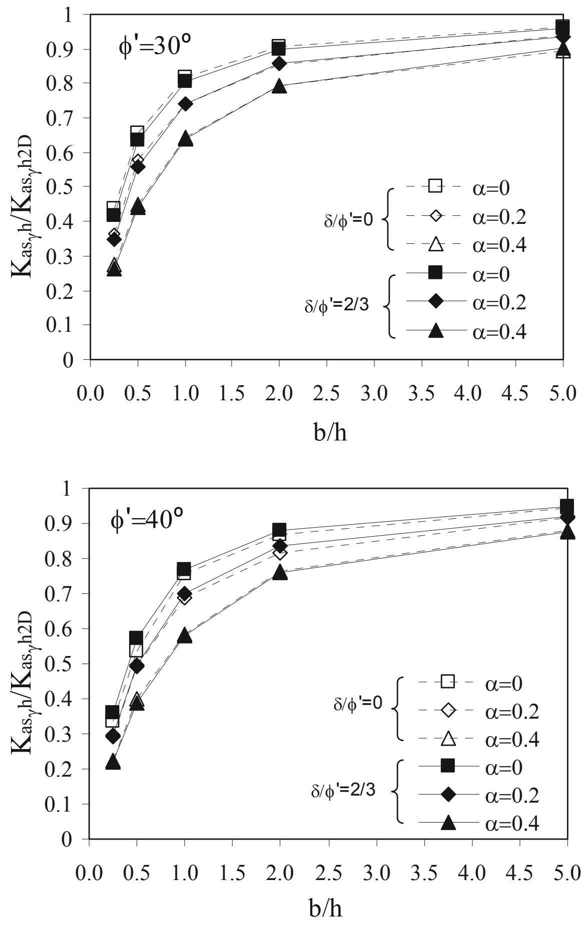

Figure 7. Values of the ratio $K_{as\gamma h}/K_{as\gamma h2D}$, as a function of b/h.

ACKNOWLEDGEMENTS

The authors would like to thank "Fundação para a Ciência e Tecnologia" (Project PTDC/ECM/70368/2006) for the financial contributions given to this paper.

REFERENCES

Antão, A. N. and Santana, T. and Vicente da Silva, M. and Guerra, N. M. C. 2011. Passive earth-pressure coefficients by upper-bound numerical limit analysis. *Canadian Geotechnical Journal* 49 (6), 651-658.

Krabbenhoft, K., Lyamin, A., Hjijaj, M., and Sloan, S. 2005. A new discontinuous upper bound limit analysis formulation. *International Journal for Numerical Methods in Engineering* 63 (7), 1069-1088.

Vicente da Silva, M. and Antão, A. N. 2008. Upper bound limit analysis with a parallel mixed finite element formulation. *International Journal of Solids and Structures* 45 (22-23), 5788-5804.

Vicente da Silva, M.; Antão, A. N.; Deusdado, N.; Vaz, D. 2012. Sublim3D – Strict Upper Bound LIMit analysis code. http://www.dec.fct.unl.pt/projectos/SUBLIM3d. December 2012.